Mechanics of Time-Dependent Materials (2025) 29:68
https://doi.org/10.1007/s11043-025-09804-w

RESEARCH

Master trends in the elasto-viscoplastic behaviour of highly cross-linked epoxy resins

Nathan Klavzer[1] · Jérémy Chevalier[2] · Christian Breite[3] · Xavier P. Morelle[4] · Yentl Swolfs[3] · Thomas Pardoen[1,5]

Received: 23 July 2024 / Accepted: 5 July 2025

Abstract
Highly cross-linked epoxy resins are ubiquitous in high-performance structural applications, particularly when used as matrices for fibre-reinforced composites. The optimisation of composites requires a quantitative and predictive description of the mechanical behaviour of the matrix. To explore master trends in the mechanical response as well as to guide first-order modelling, the complete stress-strain response of six epoxies is characterised under uniaxial compression up to large strain and fracture. A number of characteristic properties are analysed and rationalised mainly through establishing partly physical and partly empirical relationships with the ratio T/T_g of test over glass transition temperature. Among others, an enhanced Eyring-type model is identified for the yield stress and found valid for a wide range of temperatures and strain rates below T_g. The yield stress of all six epoxies is related to T_g within 10% error without any other adjustment of parameters. A similar relationship for the modulus with T/T_g also accounts for strain rate. Lastly, the failure stress and strain are found to also correlate to T/T_g in subgroups of resins with similar molecular structure, while the re-hardening modulus does not.

Keywords Polymeric material · Elastic-viscoplastic material · Mechanical testing · Glass transition temperature · Mechanical properties · Yield condition

1 Introduction

In the last few decades, the study of the elasto-viscoplastic behaviour of glassy polymers has received significant attention as a result of their omnipresence in engineering applications. Highly cross-linked thermosetting (TS) polymers, heavily used in the aeronautic and naval industries, partly suffer from a lack of in-depth investigation of their mechanical behaviour. This is based on the agreement that the general macroscale mechanical response is, to a large extent, inherently similar to that of thermoplastic polymers (TPs), except for a lower ductility on average (G'Sell and Souahi 1997; Lee 1988; Mayr et al. 1998; Oleynik 1989). The underlying assumption is that the plastic flow and the large strain behaviour in TP and TS glasses stem from a similar origin (Argon and Bessonov 1977; Yamini and Young 1980). Failure, however, appears to be inherently different. TPs often show progressive damage by crazing while TSs fail in a brittle manner due to micro-cavitation around defects (Asp et al. 1996; G'Sell and Souahi 1997; Kinloch 1989; Mayr et al. 1998; Yamini and Young 1979).

Extended author information available on the last page of the article

Published online: 01 August 2025

Most of the literature addressing the mechanical response of epoxies focuses on lowly or moderately cross-linked resins, typically based on DGEBA prepolymers and often in the context of structural adhesives.

A number of recent studies have addressed the mechanical behaviour of epoxies, both from an experimental and modelling perspective, to push towards a deeper understanding of the link between the molecular structure and properties (Gu et al. 2024; Tamrakar et al. 2018). The mechanical behaviour of highly cross-linked epoxies is impacted by the cross-linking density and by the nature of the polymer chains, on top of the test temperature, strain rate and hydrostatic pressure dependence (Cook et al. 1998; Gu et al. 2024; Moosburger-Will et al. 2013; Sindt et al. 1996; Tamrakar et al. 2018; Tian et al. 2018). In particular, the strain rate and temperature dependency of the stress-strain response is of crucial interest to understand the influence on the modulus and yield stress, but also on the re-hardening capacity. Furthermore, a strong correlation with the glass transition temperature T_g is always observed, and some authors have found clear relationships between the yield strength of TS resins and the T_g (Calzia and Lesser 2007; Fiedler et al. 2005; Lemay et al. 1984; Lesser and Calzia 2004). Physical and/or hygrothermal ageing can significantly impact the mechanical response of epoxies, particularly the yield stress (G'Sell and McKenna 1992; Odegard and Bandyopadhyay 2011). Hence, first-order correlations with T_g can be biased by such effects, complicating the analysis of the stress-strain response. To the authors' knowledge, most studies dealing with the determination of closed-form relationships between the mechanical properties of epoxies and their molecular structure or physical properties limit themselves to the analysis of the elastic modulus and yield point (in the case of compressive loads) (e.g. Behzadi and Jones 2005; Calzia and Lesser 2007).

In parallel to the disproportion in experimental studies between TPs and TSs, the modelling of the constitutive response of TSs displays a similar imbalance. While the most advanced models devoted to TPs include some strong physical grounds, models for TSs often stay at a more phenomenological level. Many studies linking the elasto-viscoplastic response of TPs with the molecular structure have indeed guided and optimised the development of advanced constitutive computational models, e.g. (Ames et al. 2009; Anand et al. 2009). The recent literature dealing with the modelling of glassy polymers, mostly on TPs, includes validation performed on only one or two systems (Barriere et al. 2019; Lan et al. 2022; Mirkhalaf et al. 2017; Park et al. 2020; Uchida et al. 2022; Wang et al. 2019; Xiao et al. 2022). One of the common characteristics of these models is a high sophistication and a large number of physical parameters. The positive outcome is a good level of predictivity but at the expense of a difficulty to separate the first and second order effects and to understand the dominant physical influences and master trends. In recent years, modelling based on molecular dynamics simulations aims at linking the mechanical properties to the fundamental molecular interactions, though many fundamental questions still remain about the exact nature of the nanoscopic plastic deformation mechanisms (a deeper description of these mechanisms is given in Sect. 2) (Khare and Phelan 2020; Konrad et al. 2021; Vu-Bac et al. 2015; Zheng et al. 2022). Plastic flow has been associated with unwinding or sliding of chain loops and dissociation of nearby links followed by binding with near fertile sites (Chen et al. 2023; Konrad et al. 2022; Radue et al. 2018; Unger et al. 2019), and can be related to fundamental reconfiguration mechanisms such as the ones proposed by Argon (Argon 1973).

Lastly, the extensive use of epoxies as matrices for polymer matrix composites (PMCs) triggered the development of multiscale characterisation strategies focused on improving the understanding of the deformation and failure of these TSs (Chevalier et al. 2019a; LLorca et al. 2013; Tan et al. 2018). The primary motivation guiding these studies is the recognition that an accurate description of the microscale deformation of epoxies is necessary to ade-

quately predict the failure of composite structures, even for simple thermoset unidirectional (UD) fibre-reinforced composites (Chevalier et al. 2019a; Hardiman et al. 2017; Pardoen et al. 2021). In many loading conditions, plastic flow within the matrix is not negligible, such as under shear, transverse compression or creep, re-emphasising the need to accurately describe the viscoplastic response beyond the onset of yielding.

Hence, there is a clear interest for the community to have access to a wider range of experimental data below T_g to serve as a basis to identify and validate advanced models. The premises of this work were to gather a vast range of elasto-viscoplastic properties resulting from compression tests on different highly cross-linked epoxy systems. The advantage of compression tests is to allow investigating the large strain behaviour without premature failure as found for epoxies deformed in tension. Experimental data at different temperatures and strain rates are extracted and rationalised with respect to the magnitude of the T_g. Care was taken to consider resins presenting a similar physical state with respect to physical ageing. The three main objectives are the following:

- To offer a rich database about the mechanical response of epoxies with a range of T_g varying over almost 200°C;
- To establish general master trends regarding the entire stress-strain response, including elasticity, yielding, softening and re-hardening, serving as a basis for first-order modelling the mechanical behaviour of epoxy systems (bulk or as used in composites);
- To rationalise regularities within the stress-strain response with respect to physico-chemical or molecular structure factors based on the current literature and to primarily link it to the T_g to provide simple robust phenomenological relationships, partly based on physics and partly purely empirical.

In particular, relationships are established to predict the modulus and yield stress of epoxies at any temperature (below T_g) and strain rate (in the low rate regime). Additionally, the re-hardening and the failure of the epoxies is related to T_g.

2 Basics on the elasto-viscoplastic behaviour of thermosets under monotonic loading

Figure 1 shows a typical true stress–true strain response of an epoxy loaded under uniaxial compression, highlighting the parameters of interest in this paper. These parameters are explained in the next paragraphs.

Upon loading, glassy polymers exhibit an elastic response with a Young's modulus E generally between 1 and 4 GPa. This initial resistance to deformation comes from secondary intermolecular interactions, mainly Van der Waals and hydrogen bonds. At larger strains, the response becomes non-linear, mainly caused by local stress relaxation due to heterogeneous molecular movements. This behaviour is temperature and strain rate dependent.

The yield point $(\varepsilon_y, \sigma_y)$ of glassy polymers has received most of the attention in the literature. This upper yield marks the transition from reversible to irreversible conformational changes in the polymer chains and is most often defined as the local maximum of the stress-strain curve. Ample experimental studies have shown that it is strongly affected by temperature, strain rate, hydrostatic pressure, thermomechanical history (i.e. ageing), relative humidity (i.e. water content of the network) and initial chain alignment (Argon 2013; Bowden 1973; Boyce et al. 1988; G'Sell 1986). Some polymer glasses also present a difference in yielding in compression and tension (Morelle et al. 2017; Poulain et al. 2014).

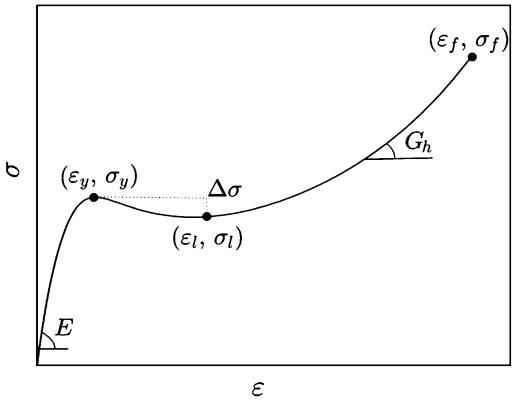

Fig. 1 Characteristic quantities of interest describing the overall elasto-visco-plastic stress-strain response of an epoxy up to failure

Ageing, whether natural or induced by the thermomechanical history of the material, leads to an increase in the yield point (Clarijs et al. 2019; Van Melick et al. 2003; Odegard and Bandyopadhyay 2011).

The strain softening regime leads to a decrease of the resistance characterised by the lower yield $(\varepsilon_l, \sigma_l)$ corresponding to the local stress minimum. The origin of intrinsic softening has yet to be fully clarified, but the consensus in the community is that it is tied to the activation of microshear domains that create local stress concentrations and promote further activation within an avalanche mechanism. Argon (2013) suggested using the concept of shear transformation zones (STZ), akin to the aforementioned microshear domains, to represent the fundamental mechanism driving the accumulation of permanent deformation. The deformation within the polymer arises from overcoming a local energy barrier of an STZ and the subsequent accumulation of such activated STZs. Similar to the upper yield point, the lower yield point is affected by temperature, strain rate and hydrostatic pressure.

The stress drop $\Delta\sigma$, defined as the difference between the upper σ_y and lower σ_l yield stresses, depends on temperature and strain rate within a specific range (Van Breemen et al. 2012), and on the degree of ageing versus rejuvenation (Meijer and Govaert 2005; Van Melick et al. 2003).

Large strain re-hardening follows after softening and the stress increases again due to the network response and chain alignment. A re-hardening modulus G_h is defined to quantify the re-hardening capacity. The re-hardening modulus has been shown to increase, decrease (Hoy and Robbins 2006; van Melick et al. 2003; Morelle 2015; Senden et al. 2012; Tervoort and Govaert 2000) or remain unchanged (Morelle 2015; Tian et al. 2018) with temperature and/or strain rate. It is also strongly affected by the network structure and the cross-linking density (van Melick et al. 2003; Tian et al. 2018). Defining G_h is not always straightforward as some systems may present continuously changing slopes in their stress-strain response. Hence, in this work, G_h is defined based on the assumption that a neo-Hookean representation is a convenient way to quantify the re-hardening response for comparative purposes despite being physically wrong (Argon 2013). This implies that the strength is proportional to $g(\lambda) = \lambda^2 - 1/\lambda$, where λ is the longitudinal stretch. Representing the stress in terms of $g(\lambda)$ means that the re-hardening part becomes linear. Hence, G_h is defined as the slope of the re-hardening part of the curve, expressed as a function of $g(\lambda)$. Note that although a large strain elasticity-based model is used to represent this part of the response (hence including elastic stiffening), it does, fundamentally, represent a strain hardening mechanism.

Several characteristics of the mechanical response of glassy polymers (e.g. elastic modulus and yield stress) can be rationalised by time-temperature superposition principles (Chen et al. 2022; Diani et al. 2015; Federico et al. 2018; Gu et al. 2024; Tamrakar et al. 2018; Zhao et al. 2024). A typical starting point is the Eyring-type approach, accounting for the temperature and strain rate (e.g. Argon 2013; Bauwens-Crowet et al. 1972; Richeton et al. 2006). The yield stress is related to the strain rate as follows:

$$\frac{\sigma_y}{T} = \frac{\Delta E}{T v_{act}} + \frac{k_b}{v_{act}} \log\left(\frac{\dot{\varepsilon}}{\varepsilon_0}\right), \tag{1}$$

where ΔE is the activation energy and v_{act} is the activation volume. The time-temperature superposition can be constructed by plotting σ_y/T as a function of $\log(\dot{\varepsilon})$ and by defining horizontal (Eq. (2)) and vertical (Eq. (3)) shift factors to generate a master curve for a specific polymer. These shift factors are defined as follows:

$$\Delta \log(\dot{\varepsilon}) = \log\left(\dot{\varepsilon}_{T_{ref}}\right) - \log\left(\dot{\varepsilon}_T\right), \tag{2}$$

$$\Delta\left(\frac{\sigma_y}{T}\right) = \frac{\sigma_y\left(T_{ref}\right)}{T_{ref}} - \frac{\sigma_y(T)}{T}. \tag{3}$$

An extended form of the Eyring-based formalism will be used to analyse some of the experimental data addressed in this paper.

3 Experimental database on highly cross-linked thermosets

In total, six epoxy-amine systems were analysed to determine the master trends in the mechanical response of this class of polymers, based on uniaxial compression tests of cylinders of height and diameter equal to 12 mm under constant strain rate. All resins were tested under well lubricated conditions, avoiding barrelling at large strains, in a screw-driven Zwick–Roell universal testing machine with a 250 [kN] external loadcell and equipped with a Wyoming Test Fixture subpress. Strain measurements were performed using a linear variational displacement transducer and correcting for machine compliance. The stress-strain responses for the epoxies at all tested temperatures and strain rates can be found in Appendix B. Table 1 presents their name, glass transition temperature and corresponding original studies. The T_g was systematically measured by differential scanning calorimetry (DSC) using similar heating rates. A precise physico-chemical description of these resins was difficult to determine as they are commercial products. The difference between systems SR8500-1 and 2 comes from the change in hardener (both amine-based). The curing cycles of each resin, which may slightly differ from the manufacturer's protocols, can be found in Appendix A. The T_g of the systems investigated in this work varies from 100°C to 287°C, namely in a range of almost 200°C, providing a relatively wide spectrum of data.

The glass transition temperature T_g will be the main physico-chemical parameter used to establish relationships valid throughout the entire database between the mechanical properties and a single characteristic of the epoxies affecting the molecular structure and deformation micromechanisms. The T_g of polymer glasses is mainly controlled by three physico-chemical factors: the functionality of the cross-links, the cross-linking density (i.e. molecular weight between cross-links) and the stiffness of the backbone of the polymer chains. It therefore represents the stiffness of the polymer network. In general, highly cross-linked epoxy systems based on high functionality precursors and amine hardeners lead to a

Table 1 Epoxy systems with corresponding glass transition temperatures and reference studies

Commercial name	Epoxy	T_g (°C)	Manufacturer	Reference data
RTM6	TGMDA	220	Hexcel (Hexcel 2022)	(Morelle 2015)
Epikote 827	DGEBA/DDS	100	Westlake Epoxy (WestlakeEpoxy 2021)	(Bahrami 2018)
Araldite MY721	TGDDM/DDS	287	Huntsman (Huntsman 2016)	(Van Velthem et al. 2021)
SR 8500-1	BA-based	105	Sicomin (Sicomin 2014)	(Breite 2021; Yu et al. 2024)
SR 8500-2	BA-based	113	Sicomin (Sicomin 2014)	(Breite 2021)
8552	TGMDA/TGAP	226	Hexcel (Hexcel 2023)	–[1]

[1]Not yet published.

densely interconnected network made of stiff aromatic-based chains, resulting in high values of T_g. In this work, all epoxy systems are amine-cured. RTM6, 8552 (TGMDA based - tetraglycidy1-4,40-methylene dianilin) and TGDDM (tetraglycidy1-4,40-diaminodiphenyl methane) are based on tetra-functional precursors, whereas SR8500-1 and 2, and DGEBA (bisphenol A diglycidyl ether) are based on di-functional precursors. TGDDM and DGEBA were cured using 4,4'-diaminodiphenyl sulfone (DDS). We will use the principle of corresponding states T/T_g to correlate the mechanical properties to T_g, instead of using the relative molecular mobility $T - T_g$. Nevertheless, both options have been shown to be equally efficient in the case of yielding (Calzia and Lesser 2007; Lemay et al. 1984). The key question at the core of the analysis to come is to determine if T_g alone is sufficient to rationalise, below T_g, the entire mechanical response up to failure of highly cross-linked epoxies or if another material/structure parameter plays a primary role on top of T_g.

Lastly, it is important to note that the reported values of σ_y correspond to naturally aged systems (i.e. with an arbitrary time between manufacturing and testing) kept at the same level of relative humidity and constant room temperature. The yield stress can be significantly reduced if rejuvenation is imposed by thermomechanical treatment. Ageing is also known to induce a slight increase in T_g (Odegard and Bandyopadhyay 2011). Nevertheless, a first study on RTM6 highly cross-linked epoxy network (and thus high T_g) has shown that the variation of σ_y is marginal despite strong accelerated aging treatment or rejuvenation (Morelle 2015). Therefore, in contrast with TPs, we suspect that in the case of highly cross-linked epoxy networks (such as the ones studied here), these effects of ageing and rejuvenation on σ_y might be hampered by the dense and rigid network. Hence, future works should also consider the comparison between rejuvenated and aged systems and its impact on the hereafter established linear relationship.

4 Results and discussion

Figure 2 shows the true stress-true strain curves at room temperature and at a true strain rate equal to 0.01 s^{-1} of all the systems addressed in this study. Evidently, the post-yield response strongly depends on the type of epoxy. In the subsequent sections, linear correlations will be established between the mechanical properties and the ratio T/T_g. The corresponding R^2 values of the regressions are systematically given.

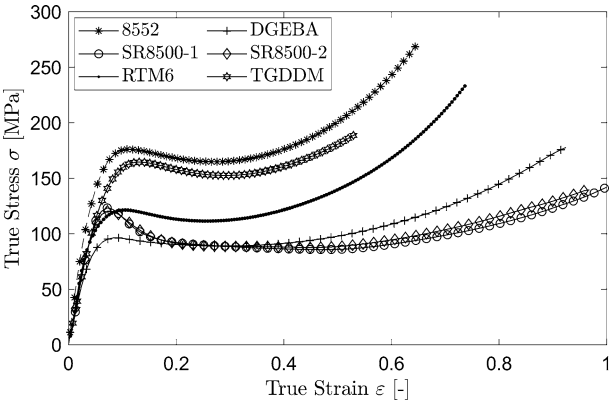

Fig. 2 True stress–true strain responses of the different epoxies at room temperature and $\dot{\varepsilon} = 0.01s^{-1}$

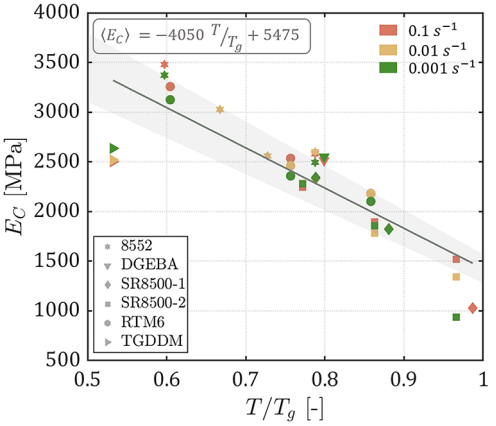

Fig. 3 Variation of the compressive Young's modulus E_C as a function of T/T_g. Each marker corresponds to a different resin. The effect of imposed strain rate is shown by the colour of the markers. The shaded area shows the $\pm 10\%$ bounds. The R^2 value of the linear regression including all data points is equal to 0.98. Coloured figure available online

4.1 Viscoelasticity

Figure 3 shows the variation of the compressive Young's modulus E_C as a function of the normalised temperature T/T_g (a brief description of the method used to determine the modulus in compression is given in Appendix C). The vertical spread within a set of data points corresponds to the effect of different imposed strain rates. The shaded area represents the $\pm 10\%$ bounds with respect to a linear regression. As expected, a decrease of temperature or an increase of strain rate leads to an increased modulus (Foreman et al. 2010; Gilat et al. 2007; Gu et al. 2024; Haward and Young 2012; Littell et al. 2008; Meijer and Govaert 2005; Poulain et al. 2014). Regardless of the strain rate, E_C linearly scales with T/T_g. The linear relationship with T/T_g is indeed expected as all systems are highly cross-linked networks based on aromatic chains; in other words, their polymer backbone nature and stiffness are rather similar. Hence, despite their differences in T_g, as a result of chemistry and cross-linking density, it is mainly the conditions of the surroundings of the chains set by the test temperature that appear to affect the modulus. This is very clear for T/T_g around 0.75–0.8 where three systems present similar moduli for similar T/T_g. The differences in molecular configuration and cross-linking density lead to variations typically less than 10% from system to system.

Nevertheless, two exceptions are worth discussing. For T/T_g higher than 0.95, the correlation fails and E_C drops significantly. This can be explained by the proximity to T_g. The

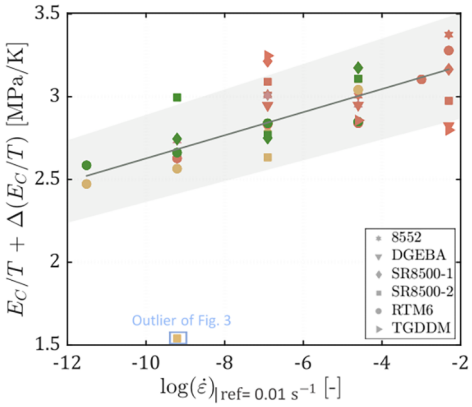

Fig. 4 Master curve of E_C/T as a function of the reference $\log(\dot{\varepsilon})$ at 0.01 s^{-1} (Eq. (2)) for all resins using a shift factor based on T_g given in Eq. (4) ($R^2 = 0.8$). The different colours for each resin represent the different test temperatures (as given in the Appendix). Coloured figure available online

glass transition is a continuous process over a specific temperature range, here defined via its mid-point T_g. Hence, for T/T_g above 0.95, the polymer systems are already partially in their transition phase, leading to a drop in the modulus to reach the value of the rubbery plateau modulus. Conversely, for TGDDM, a more compliant response shows up at lower temperatures, yet the behaviour of this polymer does not follow the master trend. Comparing the different values for different T/T_g and strain rates shows that it has an overall remarkably stable E_C as the data at different strain rates overlap. The reason for this could be found in the higher functionality of the TGDDM molecules and the inclusion of the strong sulfone dipoles, favouring the formation of hydrogen bonds. Still, this does not explain the relatively low value of the modulus.

In order to account for the temperature and strain rate simultaneously, we use the formalism described by Eqs. (1)–(3) in Sect. 2. While originally justified for the yield stress, its application to the modulus has been shown effective as well (Farotti et al. 2022). However, to also address the impact of T_g, the vertical shift factor of Eq. (3) is redefined as follows:

$$\Delta\left(\frac{E_C}{T}\right) = \frac{E_C\left(T_g\right)}{T_g} - \frac{E_C\left(T\right)}{T}, \tag{4}$$

where $E_C\left(T_g\right)$ is the modulus estimated for each resin based on the linear relationship shown in Fig. 3. The reference strain rate used for the horizontal shift is $\dot{\varepsilon} = 0.01\ s^{-1}$. Figure 4 gives the new relationship between E_C/T and $\log(\dot{\varepsilon})$. A decent fit is found, with the exception of one data point for SR8500-2. This data point was already ruled out as an outlier in the E_C versus T/T_g graph, as the test temperature is too close to the T_g of the resin. The results of Fig. 4 show that it is possible to predict the modulus within $\pm 10\%$ at different temperatures and strain rates through the knowledge of T_g only.

While correlations with T_g can be established for E_C, one must look at the factors potentially influencing the actual T_g when comparing different data sets and/or using modulus values in the literature in order to link the modulus to the molecular structure. Indeed, plastifying effects due to water (or other solvents) adsorption (Guo et al. 2021; Ito et al. 2005) as well as incomplete levels of curing (Moosburger-Will et al. 2013; Morelle 2015) strongly influence E_C via a change in T_g.

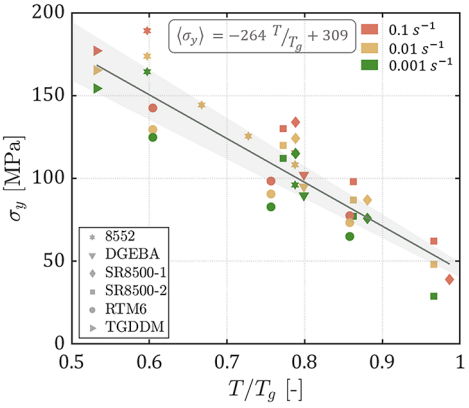

Fig. 5 Variation of the compressive upper yield stress σ_y as a function of T/T_g. $R^2 = 0.79$. Coloured figure available online

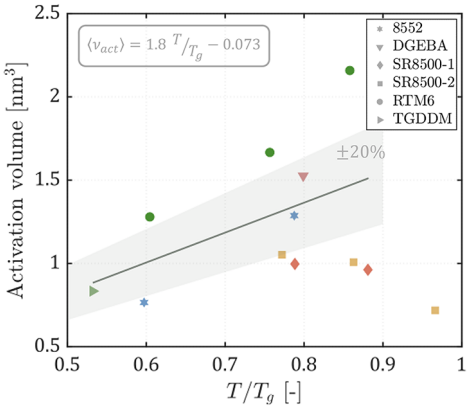

Fig. 6 Variation of the activation volume calculated in the context of an Eyring model as a function of T/T_g up to $T/T_g = 0.9$. The shaded area represents the +- 20% fit. Coloured figure available online

4.2 Onset of plastic yielding

Figure 5 presents the variation of the upper yield stress σ_y with T/T_g. The temperature and strain rate dependencies of the resins are as expected, namely an increase of σ_y as the temperature decreases or as the strain rate increases. Furthermore, a linear relationship between σ_y and T/T_g is found. The comparison with Fig. 6 (a), showing the strain rate sensitivity of the upper yield stress, confirms that all systems present a similar dependence on strain rate with respect to T/T_g. The T_g of an epoxy directly dictates its strength as it defines its molecular mobility, whether it is a mobility associated with reversible changes of configuration (i.e. elasticity in Fig. 3) or irreversible changes. From a micromechanical point of view, the origin of plastic flow is assumed to be the consequence of the nucleation of local shear events whose collaborative percolation leads to increased chain mobility, allowing for large conformational changes to occur (Argon 2013; Bowden 1973; Oleynik 1989; Quinson et al. 1997), also associated with softening, see Sect. 4.3. Hence, in general, high T_g systems require the overcoming of a larger energy barrier to initiate this chain of events. The thermomechanical plastic yielding process can be rationalised by relying on an Eyring-type formalism (see Eq. (1)). The variation of the activation volume v_{act}, entering in Eq. (1), with T/T_g is given in Fig. 6. It shows that v_{act} increases with T/T_g, with the exception of the SR8500-1/2 resins. A simple linear empirical relationship is proposed for $T/T_g < 0.9$, which writes as $v_{act}\left(T/T_g\right) = 1.8T/T_g\ - 0.073$ [nm^3]. The comparison with Fig. 5 shows

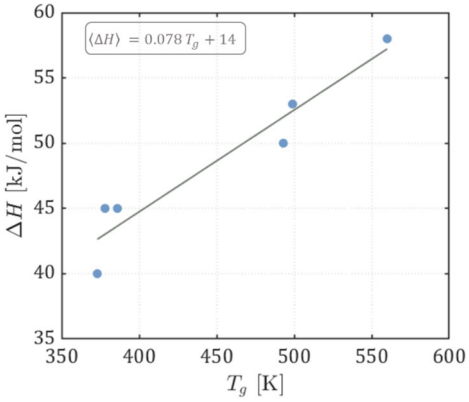

Fig. 7 Variation of the identified ΔH fitting parameter with respect to T_g

that, for each T/T_g, a higher yield stress system involves a lower activation volume. In general, the activation volume has been found to increase with temperature (Cook et al. 1998; Melot et al. 1994) and with entanglement density (Ho et al. 2003). The exception of the SR8500-1/2 resins may be due to a slightly lower cross-linking density.

Richeton et al. (2006) extended the Eyring formalism presented in Sect. 2 into the so-called cooperative model. An expression was established for relating the yield stress to the temperature and strain rate of TPs in the form:

$$\sigma_y = \sigma_i\,(0) - mT + \frac{2k_bT}{v_{act}}\sinh^{-1}\left(\frac{\dot{\varepsilon}}{\dot{\varepsilon}_0 \exp\left(\frac{\Delta H_\beta}{k_bT}\right)}\right)^{(1/n)}, \tag{5}$$

where $\dot{\varepsilon}_0$ is a constant pre-exponential factor, ΔH is the activation energy (to be fitted), $\sigma_i\,(0)$ is the athermal internal yield stress, v_{act} refers to the activation volume in Eq. (1), m is a material parameter and n is a fitting parameter.

Although Richeton et al. (2006) identified the specific material parameters of Eq. (5) for each TP under investigation, the goal here is to determine if one can find a single set of parameters either identical for all thermosets or dependent only on T_g. From the established linear relationship between σ_y and T/T_g in Fig. 5 ($\sigma_y = -264T/T_g + 309$), one can readily identify $m = 264/T_g$ MPa/K and $\sigma_i\,(0) = 309$ MPa. A curve fitting algorithm was applied to all resins, and the best values are given by $n = 6$, $\dot{\varepsilon}_0 = 10^{15}$ s^{-1}. The activation volumes are readily available from Fig. 6, depending on T/T_g. Finally, a different parameter ΔH has been identified for each resin and a dependence on T_g has been explored. Figure 7 shows that the identified values for ΔH depend linearly on T_g. Figure 8 (a) shows the σ_y/T versus $\log(\dot{\varepsilon})$ plots at different temperatures and strain rates. It compares the experimental data for σ_y with the calculated values for the yield stress based on Eq. (5). The model reproduces the experimental data very well. This is confirmed by looking at Fig. 8 (b), which plots the relative error for each data point as a function of $\log(\dot{\varepsilon})$. The error is systematically below 10%. This means that the model expressed by Eq. (5) with the identified parameters (which only depend on T_g) can predict the yield stress for many different epoxies within 10% in the range of strain rates and temperatures covered in the analysis. The final form of the enhanced Eyring model of Eq. (5) that can be used to estimate the yield stress of highly cross-linked

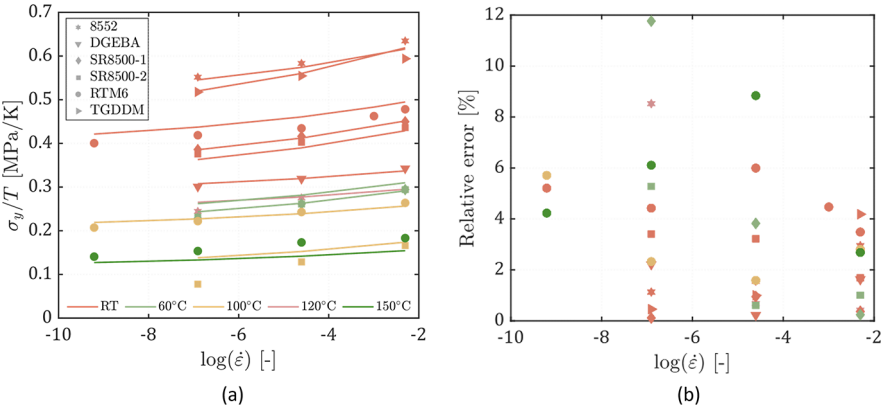

Fig. 8 (a) Variation of σ_y/T as a function of $\log(\dot{\varepsilon})$ at different temperatures and strain rates comparing the experimental values (markers) and the yield stress predicted by the enhanced Eyring's model of Eq. (5) and (b) relative error with respect to the experimental results. Coloured figure available online

thermosets (below T_g and at a strain rate below 1 s^{-1}) writes as follows:

$$\sigma_y = 309 - 264T + \frac{2k_bT}{10^{-26}\left(1.8T/T_g - 0.073\right)}\sinh^{-1}\left(\frac{\dot{\varepsilon}}{10^{15}\exp\left(\frac{10^3(0.078T_g+14)}{k_bT}\right)}\right)^{1/6} \text{[MPa]} \tag{6}$$

The fact that ΔH increases with increasing T_g as $\Delta H = 0.078\ T_g + 14$ [kJ/mol] is surprising as, in principle, only one relaxation mechanism, related to the main chain (segmental) motion, is active within the tested range of temperatures and strain rates. The addition of ΔH allows accounting for some of the non-linearity of the yield stress resulting from some potential variability between the systems. This variability seems limited, leading to a linear empirical relationship for the fitting parameter ΔH. At higher strain rates, this simple linear relationship is likely invalid as secondary processes will start partly affecting the yield behaviour (Van Breemen et al. 2012).

Early studies already attempted to relate the yield stress of epoxies to T_g (based on the control of the molecular weight between cross-links) based on $T - T_g$ and found a clear correlation (Lemay et al. 1984; Mayr et al. 1998). Hence, the correlation in Fig. 5 was expected. In addition, Calzia et al. (Calzia and Lesser 2007) demonstrated the potential to create an almost perfect linear relationship between σ_y and T/T_g for some epoxy networks by accounting for secondary factors related to the chain structure. Here, we prove that even though T_g is certainly not the only factor affecting the yield stress, it is by far the prime characteristic of highly cross-linked epoxies dictating the resistance to plastic yielding. Nevertheless, this semi-empirical model needs to be confronted to more data from the literature.

The yield strain ε_y corresponding to the onset of plasticity has not received much attention in the literature. Figure 9 shows the linear decreasing dependence of ε_y on T/T_g. Additionally, it is worth noting that higher strain rates lead to higher ε_y without any significant variations with the rate sensitivity except for TGDDM. Marano et al. (Marano and Rink 2001) studied the onset of yield in terms of the strain and found that the strain at peak yield does not necessarily coincide with the onset of plasticity. They found that, typically, the real onset of plasticity takes place beyond the peak yield. Earlier, Quinson et al. (David et al.

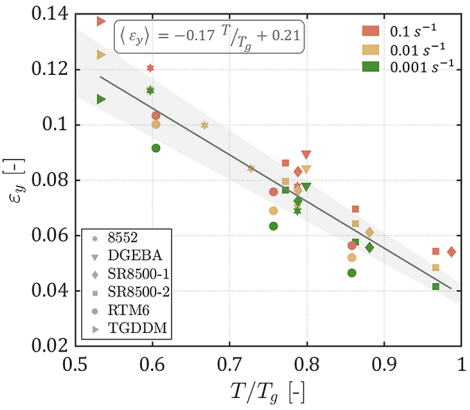

Fig. 9 Variation of the compressive upper yield strain ε_y as a function of T/T_g. $R^2 = 0.83$. Coloured figure available online

1997; Quinson et al. 1996) studied the strain component evolution for two thermoplastics and divided the total strain as the sum of three contributions: elastic, anelastic (recoverable over longer periods) and plastic. Similar results were found by Hasan and Boyce (Hasan and Boyce 1993). The anelastic strain significantly increases from the beginning and peaks around the upper yield stress level. Conversely, the plastic strain was only initiated when the stress reached σ_y. Hence, a significant portion of ε_y must be dictated by its anelastic component ε_{an}. Quinson et al. also showed that ε_{an} decreases with increasing temperature in accordance with Fig. 9. Lastly, as ε_{an} is at its highest when the stress reaches σ_y, the similarity in tendencies of Fig. 5 and Fig. 9 becomes clear.

Reconsidering the phenomenology of yielding from an STZ physical point of view, the distinction between anelastic and yield strain becomes meaningless as the macroscopic strain is then simply the consequence of the accumulation of progressive local conformation changes that bring forth the pre-peak non-linearity and the yield point (and all subsequent changes) (Chevalier et al. 2018; Lin et al. 2023; Van Loock et al. 2021; Voyiadjis and Samadi-Dooki 2016). Plastic deformation can then be interpreted as the successive percolating activation of STZs whose energy barrier to return to their initial configuration is too high to overcome without the help of external energy in the form of heat or mechanical loading.

4.3 Softening

Figure 10 illustrates how the lower yield stress σ_l scales with T/T_g. The correlation appears to be even better than for the upper yield, which could have been expected as the mechanical rejuvenation in the post-yield regime erases potential prior ageing-related effects. Naturally, both upper and lower yield stresses are closely linked and present the same dependencies on external factors. Hence, a similar dependency on T/T_g was expected. Van Breemen et al. (Van Breemen et al. 2012) offer a potential argument justifying the stronger correlation. They investigated the evolution of both the upper and lower yield stresses with temperature and strain rate of thermoplastics to determine the impact of molecular relaxation mechanisms on softening. They demonstrated that three distinct phases can exist depending on the temperature and strain rate. At high temperatures or low strain rates, both upper and lower yield stresses are only affected by α-relaxation. Then, at intermediate temperature or strain rate, the upper yield stress is affected by both α and β relaxations, while the lower yield stress remains only affected by α-relaxation. Finally, at low temperatures or high strain

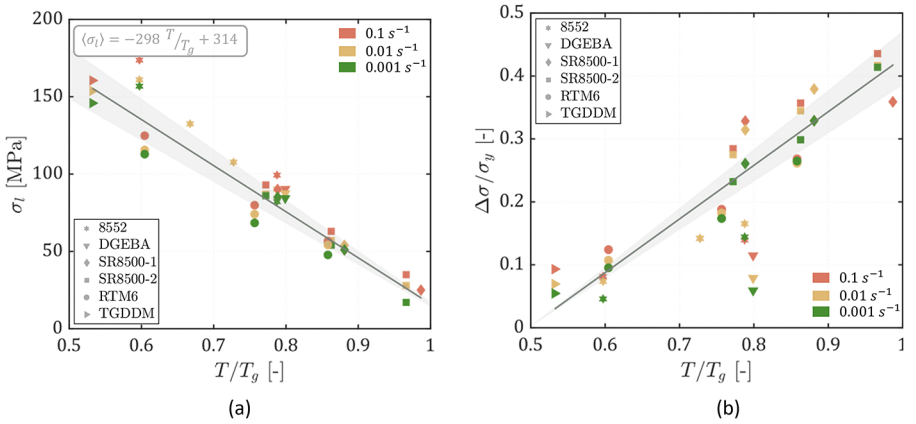

Fig. 10 Variation of (a) the compressive lower yield stress σ_l ($R^2 = 0.85$) and (b) the normalised stress drop $\Delta\sigma/\sigma_y$ as a function of T/T_g. Coloured figure available online

rates, both upper and lower yield stresses are affected by α and β relaxations. Hence, they determined that the stress drop $\Delta\sigma$ is constant only if both the upper and lower yield stresses are affected by the same mechanisms. Figure 10 (b) gives the evolution of $\Delta\sigma/\sigma_y$ for the studied epoxy systems. One can see that RTM6 is the only epoxy presenting a limited rate dependency as T/T_g increases, suggesting that the plastic flow mechanism may be affected by α relaxations only under these conditions. This implies that the aforementioned correlation for σ_y in Fig. 5 is impacted by a superposition of two relaxation mechanisms, whereas the correlation of σ_l in Fig. 10 is only affected by one and therefore correlates better with T/T_g. In addition, Fig. 10 (b) highlights that the DGEBA epoxy presents a small softening and lies outside the linear relationship. Odegard (Odegard and Bandyopadhyay 2011), G'Sell (G'Sell and McKenna 1992) and co-authors (Hasan and Boyce 1995; Kramer 2005; Van Melick et al. 2003) have shown that ageing does not significantly affect the lower yield stress. Thus, DGEBA may be in a more rejuvenated state than the other systems, as full rejuvenation of glassy polymers has been shown to suppress softening completely by reducing the amplitude of the upper yield. Ultimately, the linear relationship for σ_l emphasises an important aspect: plasticity allows these systems to find configurations that tend to suppress any other effects than the ones affecting T_g.

4.4 Re-hardening

Figure 11 illustrates the evolution of the re-hardening modulus G_h with T/T_g. While no global correlation with T/T_g can be made, three subgroups can be distinguished. Furthermore, G_h appears relatively independent of temperature for each subgroup, yet seems to be slightly impacted by the strain rate. Still, note that data for DGEBA and TGDDM correspond to one temperature only. The effect of temperature is less clear, with studies showing an increase (Hoy and Robbins 2006; van Melick et al. 2003; Senden et al. 2012) or independence on temperature (Morelle 2015; Tian et al. 2018). Additionally, the categorisation of epoxies with similar T_g into subgroups suggests that higher T_g resins also present a stronger re-hardening capacity. Indeed, the lowest group encompasses resins presenting a T_g close to 100 °C, whereas the middle group corresponds to resins with T_g above 200 °C. Van Melick (van Melick et al. 2003) suggested that G_h increases with increasing network density. More

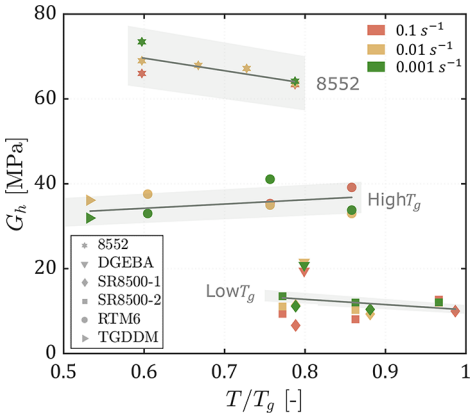

Fig. 11 Variation of the re-hardening modulus G_h as a function of T/T_g. Coloured figure available online

recently, Tian et al. (Tian et al. 2018) experimentally characterised the re-hardening of a thermoset polymer over a wide range of temperatures (going from rubbery to glassy state), strain rate and cross-linking density. They showed that, in the glassy state, G_h is almost unaffected by temperature or strain rate. Furthermore, for highly cross-linked systems, G_h is independent of the network density and the more pronounced re-hardening that is observed for such systems comes from a lower stretch capacity of the polymer chains in between cross-links. Hence, future work will consist of characterising the molecular chains of these resins, to determine their relative stretch capacity and see if it relates to T_g. The case of 8552, which shows a large G_h, can be explained by the thermoplastic toughening inclusions in the formulation, namely polyethersulfone (PES, $T_g =\sim 225°C$). While the addition of PES only slightly increases the pre-softening properties (Jung et al. 2021), its impact on G_h is significant. Lastly, it should be noted that for the high strain rate of 0.1 s^{-1}, some viscous heating can impact the stress-strain response (see Appendix B), particularly for the low T_g group. Viscous heating has been shown to affect re-hardening and, to a lesser extent, the softening behaviour (Van Breemen et al. 2012; Tamrakar et al. 2020). Here, the value of G_h of the low T_g group corresponding to 0.1 s^{-1} is systematically lower and slightly more out of trend.

Several modelling studies have shown that entropic and viscous contributions to strain re-hardening are necessary to reproduce the experimental results (Argon 2013; Hoy and Robbins 2006; Tervoort and Govaert 2000). Additionally, it appears that irreversible local conformation changes continue to occur during re-hardening. Hence, a fully neo-Hookean representation of the re-hardening capacity, albeit successful for certain polymer glasses, cannot capture all the experimental trends. In the end, the experimental and modelling studies have shown that no clear physical origin has yet been attributed to the large strain re-hardening of highly cross-linked epoxies, or glassy polymers in general. Using the idea of STZs, Voyiadjis et al. (Voyiadjis and Samadi-Dooki 2016) suggested that re-hardening results from the increased difficulty of activating new STZs.

The re-hardening process is rightly denominated “hardening” as it implies that the yield stress increases for strain hardening or kinematic hardening reasons. Hence, if one unloads and reloads the system during that stage, the stress-strain curve resumes at the point of unloading. In other words, the connection to the neo-Hookean representation, although convenient and with some physical relevance regarding chain orientation, is not, strictly speaking, representing the correct physics of plastic yielding. If there is strong re-hardening, further plastic yielding is made more difficult, which means fewer options to activate STZs and

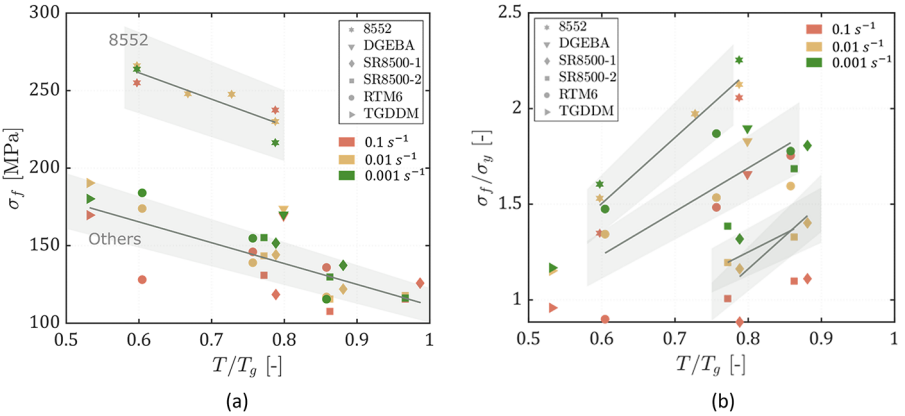

Fig. 12 Variation of (a) the failure stress σ_f and (b) the ratio σ_f/σ_y as a function of T/T_g. Coloured figure available online

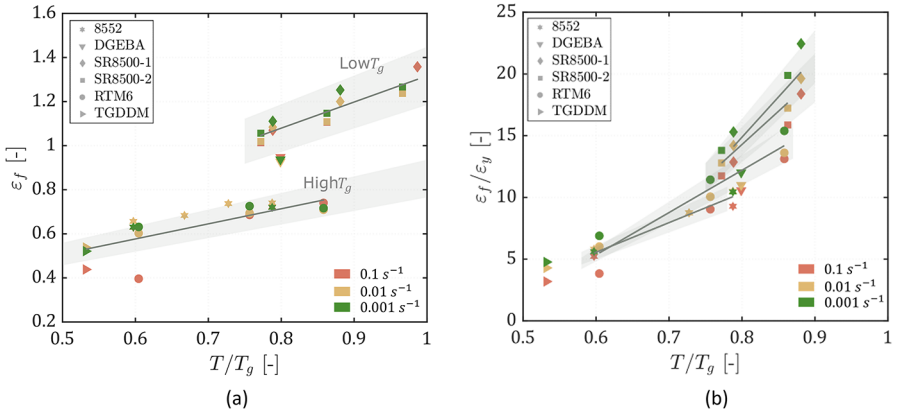

Fig. 13 Variation of (a) the failure strain ε_f and (b) the ratio $\varepsilon_f/\varepsilon_y$ as a function of T/T_g. Coloured figure available online

find regions available for configurational changes (i.e. due to the aligned elongated chain configurations).

4.5 Failure

Figure 12 (a) and Fig. 13 (a) show the dependence of the failure stress σ_f and of the failure strain ε_f on T/T_g, respectively. In both cases, linear relationships can be identified by separating the data into subgroups. For σ_f, the 8552 resin is an outlier. As mentioned in the previous section, 8552 contains tough PES inclusions increasing its re-hardening capacity and failure resistance. Still, for σ_f, setting aside 8552, the lower subgroup presents a clear correlation with T/T_g for all resins. In addition, the slope of the regression is almost equal to the one of 8552. This indeed suggests a dependency on T/T_g. However, the correlation of the subgroup is far from perfect (R^2 around 0.5). This may not be surprising as failure is in principle dictated by pre-existing defects, whose presence should not affect T_g. Chevalier et al. (2019b, 2016) extensively studied the failure of RTM6 and determined that the

Table 2 Coefficients of the linear relationships describing each property of interest with respect to T/T_g

Property γ	a	b
E_c [MPa]	−4050	5475
σ_y [MPa]	−264	309
ε_y [-]	−0.17	0.21
σ_l [MPa]	−298	314

failure is triggered by the attainment of a local critical stress value σ_c in the vicinity of an internal defect, which can be a cluster of voids (Rojek et al. 2020), both in tension and in compression (which is naturally larger than the overall σ_f value), explaining the pressure dependence of σ_f in epoxy resins. Additionally, they found that $\sigma_c = 300$ MPa and is valid for all test temperatures. In addition, the data of the low T_g resins at 0.1 s^{-1} are probably partly affected by viscous heating. Regarding ε_f, the same two subgroups as for G_h can be identified, namely the separation between higher and lower T_g systems. Each group presents a linear correlation (R^2 around 0.7) with T/T_g with similar slopes. The lower T_g resins have a higher failure strain, which appears to be related to their low re-hardening capacity. The natural explanation is that lower stress levels build up and, assuming failure is stress driven in epoxies (Chevalier et al. 2019b, 2016), larger ε_f are attained.

To put this criterion into context within this analysis, Fig. 12 (b) and Fig. 13 (b) show the dependency of the ratio σ_f/σ_y and $\varepsilon_f/\varepsilon_y$ on T/T_g, respectively. The ratio $\varepsilon_f/\varepsilon_y$ for each resin presents an increasing slope with T/T_g, partly due to the decrease of ε_y with T/T_g and partly because of the necessity to reach a critical stress condition to cause failure. In addition, the ratio σ_f/σ_y for each resin presents a similar slope with T/T_g, but shifted upwards for the higher T_g systems. Hence, the combination of lower initial yield stress at higher T/T_g and temperature independent re-hardening capacity lead to larger deformations required to locally reach the σ_c of the epoxy.

5 Final discussion and conclusion

Linear relationships have been established between several key characteristic parameters describing the mechanical response of six different epoxy resins, tested at different temperatures and strain rates, and the corresponding ratio T/T_g. The coefficients describing each property in the form of $\gamma = a\ T/T_g + b$ are summarised in Table 2 and are readily available for first-order modelling of the mechanical response of highly cross-linked epoxies solely based on the T_g and under the assumption of a limited influence of the strain rate. In addition, Eq. (4) for the modulus and Eq. (6) for the yield stress fully account for temperature and strain rate and predict the yield stress of a highly cross-linked thermoset solely based on the knowledge of the T_g.

The fact that the T_g is such a dominant marker that sets the magnitude of the elastic modulus and strength is not a surprise and can be readily understood from a molecular description of the deformation mechanisms of polymers in the glassy state. What is more surprising is that such a first-order connection with T_g also remains valid for the fracture stress. The fracture strain also follows a connection to T_g, but this connection seems to depend on the re-hardening modulus and on the factors influencing the re-hardening. The re-hardening modulus is the only parameter that cannot be rationalised with T_g. Nonetheless, the data collapse into two subgroups, based on the value of T_g suggesting a first order effect of a molecular parameter not directly influencing the magnitude of T_g. In other words, T_g

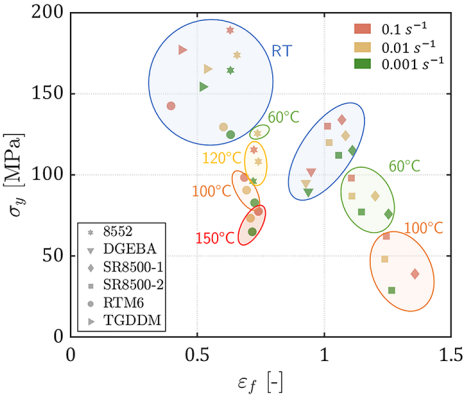

Fig. 14 Upper yield stress σ_y as a function of fracture strain ε_f for all epoxies at different strain rates and temperatures. Coloured figure available online

is very much an aggregated signature of the resistance of chain segments towards local distortion whether small and elastic or larger with some degree of irreversibility. About this last point, it is important to remember that even heavily deformed (50% or more) epoxy systems, if heated next to T_g, almost entirely recover the initial undeformed state, indicating that the "plastic" deformation is not totally irreversible like in a metal.

A question at this stage could then be to determine what is the best epoxy among all the systems that have been tested? There is no absolute answer to this question. As for almost all material classes, a larger strength (and stiffness) is accompanied by a lower fracture strain, as shown in Fig. 14, which plots σ_y as a function of ε_f. The requirements associated with different specific applications will be decided based on the constraints: the load to be carried, the maximum allowable deflection, the temperature of operation, the maximum deformation, etc. Obviously, there are systems in Fig. 14 that are clearly dominated by others, meaning with both σ_y and ε_f larger at the same temperature. One could envisage, as a next step of the analysis, applying a rational materials selection procedure following Ashby's method (Ashby 2010) to the data as, for instance, recently pursued for adhesive systems (often thermosets with lower cross-linking density) (van Innis and Pardoen 2023). However, it would then be highly relevant to pursue the present effort and extend it to the mapping of fracture toughness and fatigue resistance.

When using epoxies as matrices for composites, many recent studies have revealed the need to get a better insight into the local mechanical response at the fibre/matrix scale (Chevalier et al. 2019a; Klavzer et al. 2023; Macías et al. 2023; Mehdikhani et al. 2016). Even if globally the strains often remain small (except for specific loading conditions, such as shear), locally the matrix can reach extremely large strains, especially within tiny shear bands and characteristics such as the softening amplitude, the re-hardening modulus and the true fracture strain matter. There is still room for advanced modelling studies to understand better, using STZ models or MD simulations, the connection between molecular arrangement and configurations, the fracture strain or re-hardening modulus and the T_g. This could also guide the formulation of improved epoxy systems concerning the large strain behaviour.

Appendix A: Curing cycles of the resins

Although cure-dependent network topology changes may occur for epoxies and impact the fracture toughness, no significant variation of the stress-strain response is expected for these highly cross-linked and high T_g systems.

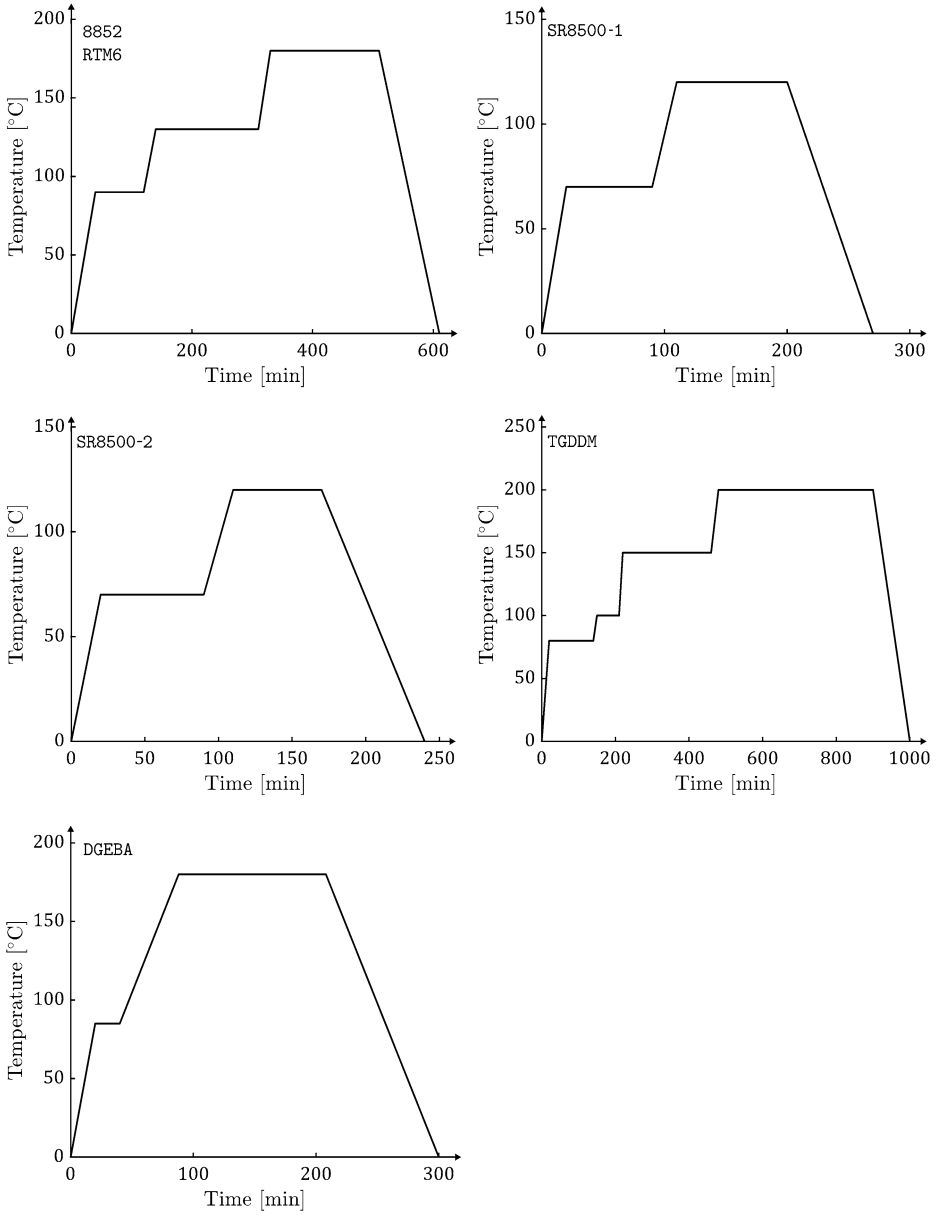

Fig. 15 Curing cycles of all the epoxy resins, which may differ from manufacturer's protocols. Refer to references in Sect. 3 for more details

Appendix B: Stress-strain curves

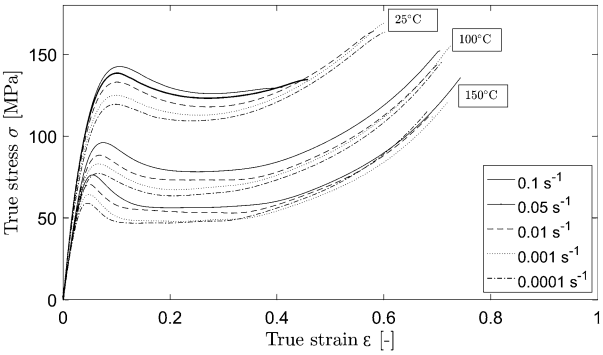

Fig. 16 Stress-strain curves for RTM6

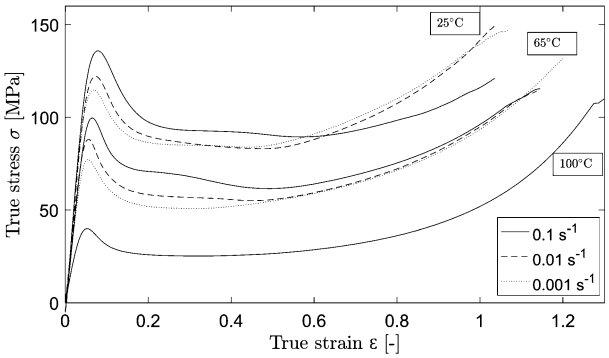

Fig. 17 Stress-strain curves for SR8500 – 1

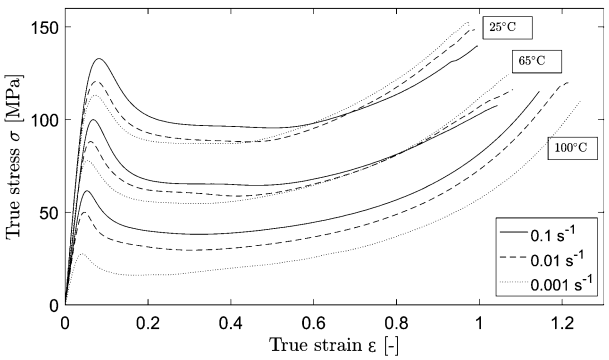

Fig. 18 Stress-strain curves for SR8500 – 2

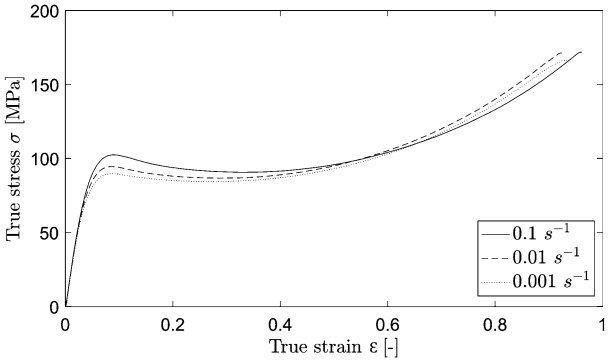

Fig. 19 Stress-strain curves for DGEBA at 25 °C

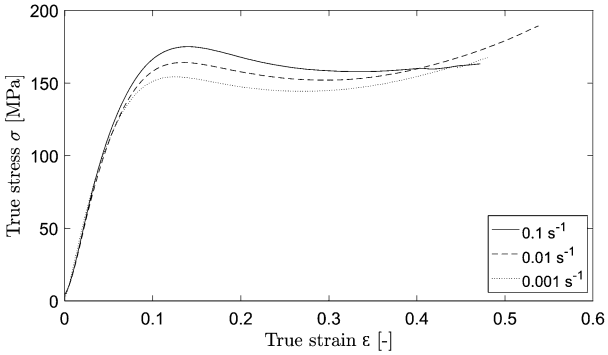

Fig. 20 Stress-strain curves for TGDDM at 25 °C

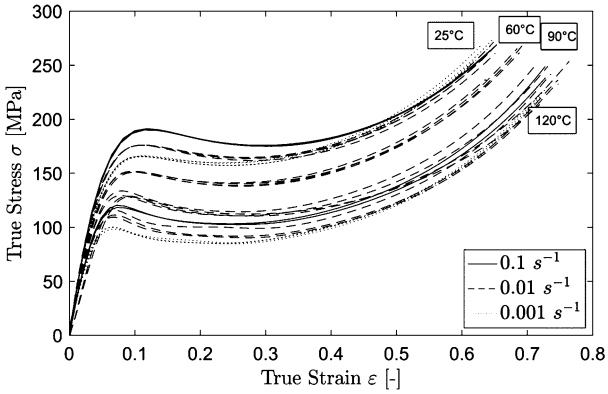

Fig. 21 Stress-strain curves for 8552

Appendix C: Determination of compression modulus

The compressive modulus has been determined following the ASTM D695 standard. A correction for the machine compliance has been systematically applied to the raw displacement data. Additionally, the initial curve toe has been corrected by applying the procedure detailed in ASTM D695, as illustrated in Fig. 22: a linear regression is made on the linear part of the stress-strain curve, which is then shifted such that the regression starts at the origin of the graph. This procedure minimises the error on the compressive modulus determination.

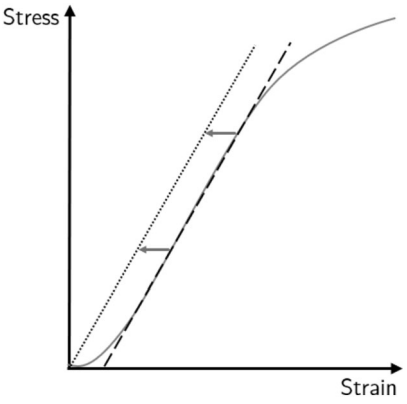

Fig. 22 Methodology to remove initial curve toe, as per ASTM D695

Acknowledgements NK is a research fellow of the Fonds de la Recherche Scientifique de Belgique - FNRS and gratefully acknowledges their support. CB kindly acknowledges the funding obtained from the Research Foundation – Flanders FWO under grant number grant agreement No 1231322N (COCOMI). The research has been partially (epoxy 8552) funded by the Walloon Region under the agreement no.7911-VISCOS in the context of the 21st SKYWIN call. The authors would like to thank the members of the LACaMI platform for providing the necessary equipment and expertise, and Wael Ballout, Pascal Van Velthem and Vincent Destoop for their support during specimen preparation. We also thank Catherine Rasse for providing aid for the statistical analysis of the data.

Author contributions N.K.: Conceptualization, Methodology, Software, Validation, Formal analysis, Investigation, Data Curation, Writing - Original Draft, Writing - Review & Editing, Visualization. J.C.: Conceptualization, Investigation, Data Curation, Writing - Review & Editing. C.B.: Conceptualization, Investigation, Data Curation, Writing - Review & Editing. X.P.M.: Conceptualization, Investigation, Data Curation, Writing - Review & Editing. Y.S.: Conceptualization, Methodology, Resources, Writing - Review & Editing, Supervision, Funding acquisition. T. P.: Conceptualization, Resources, Writing - Review & Editing, Supervision, Funding acquisition.

Data availability Data will be available upon request.

Declarations

Competing interests The authors declare no competing interests.

References

Ames, N.M., Srivastava, V., Chester, S.A., Anand, L.: A thermo-mechanically coupled theory for large deformations of amorphous polymers. Part II: Applications. Int. J. Plast. **25**, 1495–1539 (2009). https://doi.org/10.1016/J.IJPLAS.2008.11.005

Anand, L., Ames, N.M., Srivastava, V., Chester, S.A.: A thermo-mechanically coupled theory for large deformations of amorphous polymers. Part I: Formulation. Int. J. Plast. **25**, 1474–1494 (2009). https://doi.org/10.1016/j.ijplas.2008.11.004

Argon, A.S.: A theory for the low-temperature plastic deformation of glassy polymers. Philos. Mag. **28**, 839–865 (1973). https://doi.org/10.1080/14786437308220987

Argon, A.: The Physics of Deformation and Fracture of Polymers. Cambridge University Press, Cambridge (2013)

Argon, A.S., Bessonov, M.I.: Plastic flow in glassy polymers. Polym. Eng. Sci. **17**, 174–182 (1977). https://doi.org/10.1002/pen.760170306

Ashby, M.F.: Materials Selection in Mechanical Design. Butterworth-Heinemann, Oxford (2010)

Asp, L.E., Berglund, L.A., Talreja, R.: A criterion for crack initiation in glassy polymers subjected to a composite-like stress state. Compos. Sci. Technol. **56**, 1291–1301 (1996). https://doi.org/10.1016/S0266-3538(96)00090-5

Bahrami, A.: Contributions of atomic force microscopy to the mechanical property mapping of polymer blends and nanocomposites (2018)

Barriere, T., Gabrion, X., Holopainen, S.: A compact constitutive model to describe the viscoelastic-plastic behaviour of glassy polymers: comparison with monotonic and cyclic experiments and state-of-the-art models. Int. J. Plast. **122**, 31–48 (2019). https://doi.org/10.1016/J.IJPLAS.2019.05.010

Bauwens-Crowet, C., Bauwens, J.-C., Homes, G.: The temperature dependence of yield of polycarbonate in uniaxial compression and tensile tests. J. Mater. Sci. **7**, 176–183 (1972). https://doi.org/10.1007/bf00554178

Behzadi, S., Jones, F.R.: Yielding behavior of model epoxy matrices for fiber reinforced composites: effect of strain rate and temperature. J. Macromol. Sci., Phys. **44B**, 993–1005 (2005). https://doi.org/10.1080/00222340500393881

Bowden, P.B.: The Yield Behaviour of Glassy Polymers BT - The Physics of Glassy Polymers. Presented at the (1973)

Boyce, M.C., Parks, D.M., Argon, A.S.: Large inelastic deformation of glassy polymers. Part I: Rate dependent constitutive model. Mech. Mater. **7**, 15–33 (1988)

Breite, C.: Aligning Fibre Break Models for Composites with the Observable Micro-Scale Material Behaviour. PhD Thesis (2021)

Calzia, K.J., Lesser, A.J.: Correlating yield response with molecular architecture in polymer glasses. J. Mater. Sci. **42**, 5229–5238 (2007). https://doi.org/10.1007/s10853-006-1268-0

Chen, H., Song, P., Commins, T., Graham, A., Trivedi, A.R., Siviour, C.R.: Characterization and modelling of bisphenol-a type epoxy polymer over a wide range of rates and temperatures. Polymer **249**, 124860 (2022). https://doi.org/10.1016/J.POLYMER.2022.124860

Chen, F., Liu, F., Du, X.: Molecular dynamics simulation of crosslinking process and mechanical properties of epoxy under the accelerator. J. Appl. Polym. Sci. **140** (2023). https://doi.org/10.1002/app.53302

Chevalier, J., Morelle, X.P., Bailly, C., Camanho, P.P., Pardoen, T., Lani, F.: Micro-mechanics based pressure dependent failure model for highly cross-linked epoxy resins. Eng. Fract. Mech. **158**, 1–12 (2016). https://doi.org/10.1016/j.engfracmech.2016.02.039

Chevalier, J., Brassart, L., Lani, F., Bailly, C., Pardoen, T., Morelle, X.P.: Unveiling the nanoscale heterogeneity controlled deformation of thermosets. J. Mech. Phys. Solids **121**, 432–446 (2018)

Chevalier, J., Camanho, P.P., Lani, F., Pardoen, T.: Multi-scale characterization and modelling of the transverse compression response of unidirectional carbon fiber reinforced epoxy. Compos. Struct. **209**, 160–176 (2019a)

Chevalier, J., Morelle, X.P., Camanho, P.P., Lani, F., Pardoen, T.: On a unique fracture micromechanism for highly cross-linked epoxy resins. J. Mech. Phys. Solids **122**, 502–519 (2019b). https://doi.org/10.1016/j.jmps.2018.09.028

Clarijs, C.C.W.J., Kanters, M.J.W., van Erp, M.J., Engels, T.A.P., Govaert, L.E.: Predicting plasticity-controlled failure of glassy polymers: influence of stress-accelerated progressive physical aging. J. Polym. Sci., Part B, Polym. Phys. **57**, 1300–1314 (2019). https://doi.org/10.1002/polb.24870

Cook, W.D., Mayr, A.E., Edward, G.H.: Yielding behaviour in model epoxy thermosets - II. Temperature dependence. Polymer **39**, 3725–3733 (1998). https://doi.org/10.1016/S0032-3861(97)10335-4

David, L., Quinson, R., Gauthier, C., Perez, J.: The role of anelasticity in high stress mechanical response and physical properties of glassy polymers. Polym. Eng. Sci. **37**, 1633–1640 (1997). https://doi.org/10.1002/pen.11811

Diani, J., Gilormini, P., Arrieta, J.S.: Direct experimental evidence of time-temperature superposition at finite strain for an amorphous polymer network. Polymer **58**, 107–112 (2015). https://doi.org/10.1016/J.POLYMER.2014.12.045

Farotti, E., Mancini, E., Lattanzi, A., Utzeri, M., Sasso, M.: Effect of temperature and strain rate on the formation of shear bands in polymers under quasi-static and dynamic compressive loadings: proposed constitutive model and numerical validation. Polymer **245**, 124690 (2022). https://doi.org/10.1016/J.POLYMER.2022.124690

Federico, C.E., Bouvard, J.L., Combeaud, C., Billon, N.: Large strain/time dependent mechanical behaviour of PMMAs of different chain architectures. Application of time-temperature superposition principle. Polymer **139**, 177–187 (2018). https://doi.org/10.1016/J.POLYMER.2018.02.021

Fiedler, B., Hobbiebrunken, T., Hojo, M., Schulte, K.: Influence of stress state and temperature on the strength of epoxy resins. In: 11th Int. Conf. Fract 2005 ICF11., vol. 3, pp. 2271–2275 (2005)

Foreman, J.P., Behzadi, S., Porter, D., Jones, F.R.: Multi-scale modelling of the effect of a viscoelastic matrix on the strength of a carbon fibre composite. Philos. Mag. **90**, 4227–4244 (2010). https://doi.org/10.1080/14786435.2010.495361

Gilat, A., Goldberg, R.K., Roberts, G.D.: Strain rate sensitivity of epoxy resin in tensile and shear loading. J. Aerosp. Eng. **20**, 75–89 (2007). https://doi.org/10.1061/(asce)0893-1321(2007)20:2(75)

G'Sell, C.: Plastic deformation of glassy polymers: constitutive equations and macromolecular mechanisms. In: Strength of Metals and Alloys (ICSMA 7), pp. 1943–1982. Elsevier, Amsterdam (1986)

G'Sell, C., McKenna, G.B.: Influence of physical ageing on the yield response of model DGEBA/poly(propylene oxide) epoxy glasses. Polymer **33**, 2103–2113 (1992). https://doi.org/10.1016/0032-3861(92)90876-X

G'Sell, C., Souahi, A.: Influence of crosslinking on the plastic behavior of amorphous polymers at large strains. J. Eng. Mater. Technol. Trans. ASME **119**, 223–227 (1997). https://doi.org/10.1115/1.2812248

Gu, J., Bai, Y., Zhao, Z., Zhang, C.: Temperature and strain rate sensitivity of modulus and yield strength of epoxy resin under compressive loads. Polymer **295**, 126744 (2024). https://doi.org/10.1016/J.POLYMER.2024.126744

Guo, F.L., Huang, P., Li, Y.Q., Hu, N., Fu, S.Y.: Multiscale modeling of mechanical behaviors of carbon fiber reinforced epoxy composites subjected to hygrothermal aging. Compos. Struct. **256**, 113098 (2021). https://doi.org/10.1016/J.COMPSTRUCT.2020.113098

Hardiman, M., Vaughan, T.J., McCarthy, C.T.: A review of key developments and pertinent issues in nanoindentation testing of fibre reinforced plastic microstructures. Compos. Struct. **180**, 782–798 (2017). https://doi.org/10.1016/j.compstruct.2017.08.004

Hasan, O., Boyce, M.: Energy storage during inelastic deformation of glassy polymers. Polymer **34**, 5085–5092 (1993). https://doi.org/10.1016/0032-3861(93)90252-6

Hasan, O.A., Boyce, M.C.: A constitutive model for the nonlinear viscoelastic viscoplastic behavior of glassy polymers. Polym. Eng. Sci. **35**, 331–344 (1995). https://doi.org/10.1002/pen.760350407

Haward, R.N., Young, R.J.: Physics of Glassy Polymers. Springer, Dordrecht (2012)

Hexcel: HexFlow RTM6/RTM6-2 Product Data Sheet. Hexcel Corp., 1–14 (2022)

Hexcel: HexPly 8552 - Product Data Sheet (2023)

Ho, J., Govaert, L., Utz, M.: Plastic deformation of glassy polymers: correlation between shear activation volume and entanglement density. Macromolecules **36**, 7398–7404 (2003). https://doi.org/10.1021/ma025733d

Hoy, R.S., Robbins, M.O.: Strain hardening of polymer glasses: effect of entanglement density, temperature, and rate. J. Polym. Sci., Part B, Polym. Phys. **44**, 3487–3500 (2006). https://doi.org/10.1002/polb.21012

Huntsman: Technical Datasheet of Araldite MY 721 Resin. 5 (2016)

Ito, S., Hashimoto, M., Wadgaonkar, B., Svizero, N., Carvalho, R.M., Yiu, C., Rueggeberg, F.A., Foulger, S., Saito, T., Nishitani, Y., Yoshiyama, M., Tay, F.R., Pashley, D.H.: Effects of resin hydrophilicity on water sorption and changes in modulus of elasticity. Biomaterials **26**, 6449–6459 (2005). https://doi.org/10.1016/J.BIOMATERIALS.2005.04.052

Jung, H.S., Park, Y., Nah, C.W., Lee, J.C., Kim, K.Y., Lee, C.S.: Evaluation of the mechanical properties of polyether sulfone-toughened epoxy resin for carbon fiber composites. Fiber Polym. **22**, 184–195 (2021). https://doi.org/10.1007/s12221-021-9261-4

Khare, K.S., Phelan, F.R.: Integration of atomistic simulation with experiment using time-temperature superposition for a cross-linked epoxy network. Macromol. Theory Simul. **29**, 1–16 (2020). https://doi.org/10.1002/mats.201900032

Kinloch, A.J.: Relationships Between the Microstructure and Fracture Behavior of Rubber-Toughened Thermosetting Polymers (1989). Presented at the May 5

Klavzer, N., Gayot, S.F., Coulombier, M., Nysten, B., Pardoen, T.: Nanoscale digital image correlation at elementary fibre/matrix level in polymer–based composites. Composites, Part A, Appl. Sci. Manuf. **168**, 107455 (2023). https://doi.org/10.1016/j.compositesa.2023.107455

Konrad, J., Meißner, R.H., Bitzek, E., Zahn, D.: A molecular simulation approach to bond reorganization in epoxy resins: from curing to deformation and fracture. ACS Polym. Au. **1**, 165–174 (2021). https://doi.org/10.1021/acspolymersau.1c00016

Konrad, J., Pfaller, S., Zahn, D.: Multi-Scale Modelling of Plastic Deformation, Damage and Relaxation in Epoxy Resins. Polymers (Basel) **14** (2022). https://doi.org/10.3390/polym14163240

Kramer, E.J.: Open questions in the physics of deformation of polymer glasses. J. Polym. Sci., Part B, Polym. Phys. **43**, 3369–3371 (2005). https://doi.org/10.1002/polb.20639

Lan, T., Jiang, Y., Wu, P.: A thermodynamically-based constitutive theory for amorphous glassy polymers at finite deformations. Int. J. Plast. **158**, 103415 (2022). https://doi.org/10.1016/J.IJPLAS.2022.103415

Lee, S.M.: Plastic deformation in epoxy resins. In: Polymeric Materials Science and Engineering. Proceedings of the ACS Division of Polymeric Material., pp. 136–144. ACS, Washington (1988)

Lemay, J.D., Swetlin, B.J., Kelley, F.N.: Characterization of highly cross-linked polymers. Chem. Eng. News Arch. **62**, 22 (1984). https://doi.org/10.1021/cen-v062n027.p022

Lesser, A.J., Calzia, K.J.: Molecular parameters governing the yield response of epoxy-based glassy networks. J. Polym. Sci., Part B, Polym. Phys. **42**, 2050–2056 (2004). https://doi.org/10.1002/polb.20090

Lin, J., Qian, J., Xie, Y., Wang, J., Xiao, R.: A mean-field shear transformation zone theory for amorphous polymers. Int. J. Plast. **163**, 103556 (2023). https://doi.org/10.1016/J.IJPLAS.2023.103556

Littell, J.D., Ruggeri, C.R., Goldberg, R.K., Roberts, G.D., Arnold, W.A., Binienda, W.K.: Measurement of epoxy resin tension, compression, and shear stress–strain curves over a wide range of strain rates using small test specimens. J. Aerosp. Eng. **21**, 162–173 (2008). https://doi.org/10.1061/(asce)0893-1321(2008)21:3(162)

LLorca, J., González, C., Molina-Aldareguía, J.M., Lópes, C.S.: Multiscale modeling of composites: toward virtual testing ... and beyond. JOM **65**, 215–225 (2013)

Macías, J., Arteiro, A., Otero, F., Camanho, P.P., Reinoso, J.: Micro-mechanical analysis of composite materials using phase-field models of brittle fracture. Eur. J. Mech. A Solids **102**, 105069 (2023). https://doi.org/10.1016/j.euromechsol.2023.105069

Marano, C., Rink, M.: Shear yielding threshold and viscoelasticity in an amorphous glassy polymer: a study on a styrene-acrylonitrile copolymer. Polymer **42**, 2113–2119 (2001). https://doi.org/10.1016/S0032-3861(00)00570-X

Mayr, A.E., Cook, W.D., Edward, G.H.: Yielding behaviour in model epoxy thermosets - I. Effect of strain rate and composition. Polymer **39**, 3719–3724 (1998). https://doi.org/10.1016/S0032-3861(97)10334-2

Mehdikhani, M., Aravand, M., Sabuncuoglu, B., Callens, M.G., Lomov, S.V., Gorbatikh, L.: Full-field strain measurements at the micro-scale in fiber-reinforced composites using digital image correlation. Compos. Struct. **140**, 192–201 (2016)

Meijer, H.E.H., Govaert, L.E.: Mechanical performance of polymer systems: the relation between structure and properties. Prog. Polym. Sci. **30**, 915–938 (2005). https://doi.org/10.1016/j.progpolymsci.2005.06.009

Melot, D., Escaig, B., Lefebvre, J.M., Eustache, R.P., Lauprêtre, F.: Mechanical properties of unsaturated polyester resins in relation to their chemical structure: 2. Plastic deformation behavior. J. Polym. Sci., Part B, Polym. Phys. **32**, 1805–1811 (1994). https://doi.org/10.1002/polb.1994.090321102

Mirkhalaf, S.M., Andrade Pires, F.M., Simoes, R.: Modelling of the post yield response of amorphous polymers under different stress states. Int. J. Plast. **88**, 159–187 (2017). https://doi.org/10.1016/J.IJPLAS.2016.10.008

Moosburger-Will, J., Greisel, M., Sause, M.G.R., Horny, R., Horn, S.: Influence of partial cross-linking degree on basic physical properties of RTM6 epoxy resin. J. Appl. Polym. Sci. **130**, 4338–4346 (2013). https://doi.org/10.1002/app.39722

Morelle, X.: Mechanical characterization and physics-based modeling of highly-crosslinked epoxy resin (2015)

Morelle, X.P., Chevalier, J., Bailly, C., Pardoen, T., Lani, F.: Mechanical characterization and modeling of the deformation and failure of the highly crosslinked RTM6 epoxy resin. Mech. Time-Depend. Mater. **21**, 419–454 (2017)

Odegard, G.M., Bandyopadhyay, A.: Physical aging of epoxy polymers and their composites. J. Polym. Sci., Part B, Polym. Phys. **49**, 1695–1716 (2011). https://doi.org/10.1002/polb.22384

Oleynik, E.: Plastic deformation and mobility in glassy polymers. Relax. Polym., 140–150 (1989). https://doi.org/10.1007/bfb0115425

Pardoen, T., Klavzer, N., Gayot, S., Van Loock, F., Chevalier, J., Morelle, X., Destoop, V., Lani, F., Camanho, P., Brassart, L., Nysten, B., Bailly, C.: Nanomechanics serving polymer-based composite research. C. R. Phys. **22**, 1–22 (2021). https://doi.org/10.5802/crphys.56

Park, C., Jung, J., Yun, G.J.: Multiscale micromorphic theory compatible with MD simulations in both time-scale and length-scale. Int. J. Plast. **129**, 102680 (2020). https://doi.org/10.1016/J.IJPLAS.2020.102680

Poulain, X., Benzerga, A.A., Goldberg, R.K.: Finite-strain elasto-viscoplastic behavior of an epoxy resin: experiments and modeling in the glassy regime. Int. J. Plast. **62**, 138–161 (2014). https://doi.org/10.1016/j.ijplas.2014.07.002

Quinson, R., Perez, J., Rink, M., Pavan, A.: Components of non-elastic deformation in amorphous glassy polymers. J. Mater. Sci. **31**, 4387–4394 (1996). https://doi.org/10.1007/BF00356465

Quinson, R., Perez, J., Rink, M., Pavan, A.: Yield criteria for amorphous glassy polymers. J. Mater. Sci. **32**, 1371–1379 (1997). https://doi.org/10.1023/A:1018525127466

Radue, M.S., Jensen, B.D., Gowtham, S., Klimek-McDonald, D.R., King, J.A., Odegard, G.M.: Comparing the mechanical response of di-, tri-, and tetra-functional resin epoxies with reactive molecular dynamics. J. Polym. Sci., Part B, Polym. Phys. **56**, 255–264 (2018). https://doi.org/10.1002/polb.24539

Richeton, J., Ahzi, S., Vecchio, K.S., Jiang, F.C., Adharapurapu, R.R.: Influence of temperature and strain rate on the mechanical behavior of three amorphous polymers: Characterization and modeling of the compressive yield stress. Int. J. Solids Struct. **43**, 2318–2335 (2006). https://doi.org/10.1016/j.ijsolstr.2005.06.040

Rojek, J., Breite, C., Swolfs, Y., Laiarinandrasana, L.: Void growth measurement and modelling in a thermosetting epoxy resin using SEM and tomography techniques. Contin. Mech. Thermodyn. **32**, 471–488 (2020). https://doi.org/10.1007/s00161-020-00865-5

Senden, D.J.A., Krop, S., Van Dommelen, J.A.W., Govaert, L.E.: Rate- and temperature-dependent strain hardening of polycarbonate. J. Polym. Sci., Part B, Polym. Phys. **50**, 1680–1693 (2012). https://doi.org/10.1002/polb.23165

Sicomin: In: Technical Datasheet SiPreg SR 8500 / KTA 31x, vol. 33, pp. 29–34 (2014)

Sindt, O., Perez, J., Gerard, J.F.: Molecular architecture-mechanical behaviour relationships in epoxy networks. Polymer **37**, 2989–2997 (1996). https://doi.org/10.1016/0032-3861(96)89396-7

Tamrakar, S., Ganesh, R., Sockalingam, S., Haque, B.Z., Gillespie, J.W.: Experimental investigation of strain rate and temperature dependent response of an epoxy resin undergoing large deformation. J. Dyn. Behav. Mater. **4**, 114–128 (2018). https://doi.org/10.1007/s40870-018-0144-8

Tamrakar, S., Ganesh, R., Sockalingam, S., Haque, B.Z., Gillespie, J.W.: Strain rate-dependent large deformation inelastic behavior of an epoxy resin. J. Compos. Mater. **54**, 71–87 (2020). https://doi.org/10.1177/0021998319859054

Tan, W., Naya, F., Yang, L., Chang, T., Falzon, B.G., Zhan, L., Molina-Aldareguía, J.M., González, C., Llorca, J.: The role of interfacial properties on the intralaminar and interlaminar damage behaviour of unidirectional composite laminates: experimental characterization and multiscale modelling. Composites, Part B, Eng. **138**, 206–221 (2018). https://doi.org/10.1016/j.compositesb.2017.11.043

Tervoort, T.A., Govaert, L.E.: Strain-hardening behavior of polycarbonate in the glassy state. J. Rheol. **44**, 1263–1277 (2000). https://doi.org/10.1122/1.1319175

Tian, C., Xiao, R., Guo, J.: An experimental study on strain hardening of amorphous thermosets: effect of temperature, strain rate, and network density. J. Appl. Mech. Trans. ASME **85**, 1–8 (2018). https://doi.org/10.1115/1.4040692

Uchida, M., Kamimura, K., Yoshida, T., Kaneko, Y.: Viscoelastic-viscoplastic modeling of epoxy based on transient network theory. Int. J. Plast. **153**, 103262 (2022). https://doi.org/10.1016/J.IJPLAS.2022.103262

Unger, R., Exner, W., Arash, B., Rolfes, R.: Non-linear viscoelasticity of epoxy resins: molecular simulation-based prediction and experimental validation. Polymer **180**, 121722 (2019). https://doi.org/10.1016/J.POLYMER.2019.121722

Van Breemen, L.C.A., Engels, T.A.P., Klompen, E.T.J., Senden, D.J.A., Govaert, L.E.: Rate- and temperature-dependent strain softening in solid polymers. J. Polym. Sci., Part B, Polym. Phys. **50**, 1757–1771 (2012). https://doi.org/10.1002/polb.23199

van Innis, C., Pardoen, T.: Thickness-dependent selection of adhesive joints. J. Adhes. **00**, 1–54 (2023). https://doi.org/10.1080/00218464.2023.2294131

Van Loock, F., Brassart, L., Pardoen, T.: Implementation and calibration of a mesoscale model for amorphous plasticity based on shear transformation dynamics. Int. J. Plast. **145**, 103079 (2021). https://doi.org/10.1016/J.IJPLAS.2021.103079

van Melick, H.G.H., Govaert, L.E., Meijer, H.E.H.: On the origin of strain hardening in glassy polymers. Polymer **44**, 2493–2502 (2003). https://doi.org/10.1016/S0032-3861(03)00112-5

Van Melick, H.G.H., Govaert, L.E., Meijer, H.E.H.: Localisation phenomena in glassy polymers: influence of thermal and mechanical history. Polymer **44**, 3579–3591 (2003). https://doi.org/10.1016/S0032-3861(03)00089-2

Van Velthem, P., Gabriel, S., Pardoen, T., Bailly, C., Ballout, W.: Synergy between phenoxy and CSR tougheners on the fracture toughness of highly cross-linked epoxy-based composites. Polymers (Basel) **13**, 1–16 (2021). https://doi.org/10.3390/polym13152477

Voyiadjis, G.Z., Samadi-Dooki, A.: Constitutive modeling of large inelastic deformation of amorphous polymers: free volume and shear transformation zone dynamics. J. Appl. Phys. **119**, 225104 (2016)

Vu-Bac, N., Bessa, M.A., Rabczuk, T., Liu, W.K.: A multiscale model for the quasi-static thermo-plastic behavior of highly cross-linked glassy polymers. Macromolecules **48**, 6713–6723 (2015). https://doi.org/10.1021/acs.macromol.5b01236

Wang, J., Peng, L.F., Deng, Y.J., Lai, X.M., Fu, M.W., Ni, J.: A finite strain thermodynamically-based constitutive modeling and analysis of viscoelastic-viscoplastic deformation behavior of glassy polymers. Int. J. Plast. **122**, 135–163 (2019). https://doi.org/10.1016/J.IJPLAS.2019.06.013

WestlakeEpoxy: Technical Data Sheet - EPON Resin 827 Product (2021)

Xiao, R., Tian, C., Xu, Y., Steinmann, P.: Thermomechanical coupling in glassy polymers: an effective temperature theory. Int. J. Plast. **156**, 103361 (2022). https://doi.org/10.1016/J.IJPLAS.2022.103361

Yamini, S., Young, R.J.: Crack propagation in and fractography of epoxy resins. J. Mater. Sci. **14**, 1609–1618 (1979). https://doi.org/10.1007/BF00569280

Yamini, S., Young, R.J.: The mechanical properties of epoxy resins - Part 1: Mechanisms of plastic deformation. J. Mater. Sci. **15**, 1814–1822 (1980)

Yu, J., Breite, C., Van Loock, F., Pardoen, T., Swolfs, Y.: Experimental investigation of yield and hysteresis behaviour of an epoxy resin under cyclic compression in the large deformation regime. Express Polym. Lett. **18**, 133–143 (2024). https://doi.org/10.3144/expresspolymlett.2024.11

Zhao, W., Xiao, R., Steinmann, P., Pfaller, S.: Time–temperature correlations of amorphous thermoplastics at large strains based on molecular dynamics simulations. Mech. Mater. **190**, 104926 (2024). https://doi.org/10.1016/J.MECHMAT.2024.104926

Zheng, X., Guo, Y., Douglas, J.F., Xia, W.: Competing effects of cohesive energy and cross-link density on the segmental dynamics and mechanical properties of cross-linked polymers. Macromolecules **55**, 9990–10004 (2022). https://doi.org/10.1021/acs.macromol.2c01719

Authors and Affiliations

Nathan Klavzer[1] · Jérémy Chevalier[2] · Christian Breite[3] · Xavier P. Morelle[4] · Yentl Swolfs[3] · Thomas Pardoen[1,5]

✉ N. Klavzer
nathan.klavzer@uclouvain.be

✉ T. Pardoen
thomas.pardoen@uclouvain.be

J. Chevalier
jeremy.chevalier@syensqo.com

C. Breite
christian.breite@kuleuven.be

X.P. Morelle
xavier.morelle@insa-lyon.fr

Y. Swolfs
yentl.swolfs@kuleuven.be

1 Institute of Mechanics, Materials and Civil engineering (iMMC), UCLouvain, Louvain-la-Neuve, Belgium

[2] Syensqo, Material Science Application Center (MSAC), Bruxelles, Belgium

[3] Department of Materials Engineering, KU Leuven, Leuven, Belgium

[4] Laboratoire d'Ingénierie des Matériaux Polymères – UMR CNRS 5223 – INSA de Lyon, Villeurbanne, France

[5] WEL Research Institute, Wavre, Belgium